



KEPUTUSAN DEKAN FAKULTAS TEKNOLOGI INFORMASI UNIVERSITAS BUDI LUHUR

NOMOR : K/UBL/FTI/000/002/09/25

TENTANG:

PENUGASAN KEGIATAN TRI DHARMA & PENUNJANG BAGI DOSEN FAKULTAS TEKNOLOGI INFORMASI UNIVERSITAS BUDI LUHUR SEMESTER GASAL TAHUN AKADEMIK 2025/2026

DEKAN FAKULTAS TEKNOLOGI INFORMASI UNIVERSITAS BUDI LUHUR

- Menimbang : 1) Bahwa Dosen adalah pendidik profesional dan ilmu dengan tugas utama mentrans-formasikan, mengembangkan, dan menyebarkan ilmu pengetahuan, teknologi, dan seni melalui pendidikan/pengajaran penelitian & karya ilmiah, dan Pengabdian pada masyarakat yang dikenal dengan istilah Tri Dharma Perguruan Tinggi;
- 2) Bahwa untuk meningkatkan profesionalitas dan kompetensi sebagai pendidik profesional maka dipandang perlu untuk memberikan tugas-tugas tambahan/penunjang dalam lingkup kegiatan penunjang Tri Dharma;
- Mengingat : 1) Undang – undang Republik Indonesia Nomor 12 Tahun 2012 tentang Pendidikan Tinggi;
- 2) Undang – undang Republik Indonesia Nomor 20 tahun 2003 tentang Sistem Pendidikan Nasional;
- 3) Peraturan Pemerintah Republik Indonesia Nomor 17 Tahun 2010 tentang Pengelolaan dan Penyelenggaraan Pendidikan;
- 4) Peraturan Menteri Riset, Teknologi, dan Pendidikan Tinggi Republik Indonesia Nomor 53 Tahun 2023 tentang Penjaminan Mutu Perguruan Tinggi;
- 5) Keputusan Ketua Yayasan Pendidikan Budi Luhur Cakti Nomor: K/YBLC/KEP/000/216/06/2023 tentang Statuta Universitas Budi Luhur;
- 6) SK YPBLC No: K/YBLC/KEP/000/020/01/24 tanggal 05 Januari 2024 tentang Pengangkatan Para Pejabat Struktural Universitas Budi Luhur Periode 2024-2028
- MEMUTUSKAN**
- Menetapkan :
PERTAMA : Menugaskan dosen-dosen Fakultas Teknologi Informasi Universitas Budi Luhur untuk melaksanakan kegiatan **Tri Dharma Perguruan Tinggi dan penunjangnya** pada Semester Gasal Tahun Akademik 2025/2026 yang meliputi:
- a. **Kegiatan partisipasi aktif** dalam Pertemuan Ilmiah sebagai Ketua/Anggota/Peserta/Pembicara/Penulis/Narasumber pada kegiatan Seminar, Workshop, Konferensi, Pelatihan, Simposium, Lokakarya, Forum Diskusi, Sarasehan dan sejenisnya;
- b. **Publikasi Ilmiah** pada Prosiding, Jurnal/majalah/surat kabar dan sejenisnya;
- c. **Partisipasi dalam organisasi** profesi, organisasi keilmuan dan/atau organisasi lain yang menunjang kegiatan Tri Dharma Pendidikan Tinggi;
- d. **Pengabdian Kepada Masyarakat (PPM)**, dalam kegiatan terprogram, terjadwal atau insidental;
- KEDUA : Dosen-dosen yang melaksanakan penugasan wajib membuat Laporan Kegiatan, dengan mengikuti pedoman dari Fakultas/Program Studi, sebagai pertanggungjawaban atas kegiatan yang diikuti;
- KETIGA : Kegiatan Tri Dharma yang tidak termasuk dalam surat keputusan ini akan memiliki penugasan tersendiri;
- KEEMPAT : Keputusan ini berlaku sejak tanggal ditetapkan dan akan diubah sebagaimana mestinya apabila di kemudian hari terdapat kekeliruan.

Ditetapkan di : Jakarta

Tanggal : 02 September 2025

Dekan Fakultas Teknologi Informasi



Dr. Ir. Achmad Solichin, S.Kom., M.T.I



**LAMPIRAN KEPUTUSAN DEKAN FAKULTAS TEKNOLOGI INFORMASI
UNIVERSITAS BUDI LUHUR**

NOMOR : K/UBL/FTI/000/002/09/25

**TENTANG:
PENUGASAN KEGIATAN TRI DHARMA & PENUNJANG BAGI DOSEN
FAKULTAS TEKNOLOGI INFORMASI UNIVERSITAS BUDI LUHUR
SEMESTER GASAL TAHUN AKADEMIK 2025/2026**

No	NUPTK	Nama	Program Studi
1	6356750651130093	ABDUL MUIS SOBRI	Teknik Informatika (S1)
2	5934758659137112	ACHMAD ADITYA ASHADUL USHUD	Teknik Informatika (S1)
3	4437767668130323	ACHMAD ARDIANSYAH	Teknik Informatika (S1)
4	7937760661130282	ACHMAD SOLICHIN	Ilmu Komputer (S3)
5	5454763664230162	AGNES ARYASANTI	Sistem Informasi (S1)
6	1947743644130112	AGUNG PRIHARTONO	Sistem Informasi (S1)
7	4652761662130272	AGUNG SAPUTRA	Teknik Informatika (S1)
8	8141761662130183	AGUS UMAR HAMDANI	Sistem Informasi (S1)
9	2636769670130302	AHMAD PUDOLI	Teknik Informatika (S1)
10	3955753654130082	AKHMAD UNGGUL PRIANTORO	Ilmu Komputer (S2)
11	1653757658130122	ANDY RIO HANDOKO	Teknik Informatika (S1)
12	1646766667130292	ANGGA KUSUMA NUGRAHA	Teknik Informatika (S1)
13	8947761662230262	ANITA DIANA	Sistem Informasi (S1)
14	0544751652130173	ANTON SATRIA PRABUWONO	Ilmu Komputer (S2)
15	4535772673130233	ANWAR RIFA'I	Teknik Informatika (S1)
16	5060770671130293	AQMAL MAULANA	Teknik Informatika (S1)
17	6647764665131142	ARI SAPUTRO	Manajemen Informatika (D3)
18	5239757658130173	ARIEF WIBOWO	Ilmu Komputer (S3)
19	0543756657130133	ARIF BRAMANTORO	Ilmu Komputer (S2)
20	4162753654131073	ARMAN YUSUF	Teknik Informatika (S1)
21	2533753654130132	ARSANTO NARENDRO	Teknik Informatika (S1)
22	5251757658130183	ASEP ABDUL ROHMAN	Sistem Informasi (S1)
23	7752762663237012	ATIK ARIESTA	Manajemen Informatika (D3)
24	3733759660130242	BASUKI HARI PRASETYO	Teknik Informatika (S1)
25	9846770671130352	BAYU SATRIA PRATAMA	Sistem Informasi (S1)
26	9551750651130082	BRURI TRYA SARTANA	Sistem Informasi (S1)
27	2555742643130063	BULLION DRAGON ANDAH	Sistem Informasi (S1)
28	3251756657130123	DARMAWAN BAGINDA NAPITUPULU	Ilmu Komputer (S2)
29	5560751652130083	DENI MAHDIANA	Sistem Informasi (S1)



No	NUPTK	Nama	Program Studi
30	8556757658137103	DENNI KURNIAWAN	Ilmu Komputer (S2)
31	3535770671130233	DEVIT SETIONO	Sistem Informasi (S1)
32	1542762663230293	DEWI KUSUMANINGSIH	Sistem Informasi (S1)
33	4454761662130162	DIAN ANUBHAKTI	Sistem Informasi (S1)
34	7637741642130122	DJATI KUSDIARTO	Sistem Informasi (S1)
35	2243767668130313	DOLLY VIRGIAN SHAKA YUDHA SAKTI	Teknik Informatika (S1)
36	4556758659231082	DWI PEBRIANTI	Ilmu Komputer (S2)
37	9560763664230232	DWI PUSPITA ANGGRAENI	Teknik Informatika (S1)
38	2155762663131103	FERDIANSYAH	Komputerisasi Akuntansi (D3)
39	3453751652130073	FX BIMA CAHYA PUTRA	Sistem Informasi (S1)
40	2538753654130102	GANDUNG TRIYONO	Sistem Informasi (S1)
41	9043744645130083	GATOT PURWANTO	Sistem Komputer (S1)
42	4751753654230082	GRACE GATA	Komputerisasi Akuntansi (D3)
43	0537746647130122	GUNAWAN PRIA UTAMA	Teknik Informatika (S1)
44	0740763664130282	HADIDTYO WISNU WARDANI	Teknik Informatika (S1)
45	5846747648130102	HARI SOETANTO	Ilmu Komputer (S3)
46	9838763664130292	HARIS MUNANDAR	Teknik Informatika (S1)
47	8857759660131082	HENDRI IRAWAN	Sistem Informasi (S1)
48	0652765666130282	HILLMAN AKHYAR DAMANIK	Teknik Informatika (S1)
49	4735758659130162	HUMISAR HASUGIAN	Sistem Informasi (S1)
50	0434764665230262	IKA SUSANTI	Teknik Informatika (S1)
51	8949771672130282	IKHSAN RAHDIANA	Teknik Informatika (S1)
52	3941771672130302	IMAN PERMANA	Sistem Komputer (S1)
53	7437754655230112	IMELDA	Teknik Informatika (S1)
54	7746771672230342	INDAH PUSPASARI HANDAYANI	Sistem Informasi (S1)
55	2654764665130222	INDRA	Teknik Informatika (S1)
56	7454765666130203	INDRA HERTANTO	Teknik Informatika (S1)
57	9950765666130302	INDRA NUGRAHA ABDULLAH	Ilmu Komputer (S2)
58	0537752653130122	IRAWAN	Sistem Komputer (S1)
59	6435760661230183	ITA NOVITA	Sistem Informasi (S1)
60	7734743644130092	JAN EVERHARD RIWUROHI	Ilmu Komputer (S3)
61	1944770671130422	JEREMY JONATHAN	Sistem Informasi (S1)
62	9456761662130143	JOKO CHRISTIAN	Manajemen Informatika (D3)
63	2935754655130132	JOKO SUTRISNO	Sistem Informasi (S1)
64	2851769670130282	KUKUH HARSANTO	Sistem Informasi (S1)
65	9849754655130112	LAUW LI HIN	Sistem Informasi (S1)



UNIVERSITAS BUDI LUHUR

FAKULTAS TEKNOLOGI INFORMASI

KAMPUS PUSAT : Jl. Raya Ciledug, Petungkang Utara, Jakarta Selatan 12260

Telp : (021) 5853753 (Hunting) Fax : (021) 7471164, 5853752

Website : <http://www.budiluhur.ac.id>

No	NUPTK	Nama	Program Studi
66	5460755656230082	LESTARI MARGATAMA	Teknik Informatika (S1)
67	6849759660131132	LIS SURYADI	Komputerisasi Akuntansi (D3)
68	3457756657130123	LUHUR BAYUAJI	Ilmu Komputer (S2)
69	1654747648130072	MARDI HARDJIANTO	Ilmu Komputer (S2)
70	8639765666237002	MARINI	Sistem Informasi (S1)
71	5540767668230303	MEPA KURNIASIH	Teknik Informatika (S1)
72	4562753654230103	MERRY ANGGRAENI	Teknik Informatika (S1)
73	2453748649130073	MOHAMMAD ANIF	Teknik Informatika (S1)
74	9248752653130093	MOHAMMAD SYAFRULLAH	Ilmu Komputer (S2)
75	0643760661230242	MOTIKA DIAN ANGGRAENI	Sistem Informasi (S1)
76	2961757659200032	MUFTI	Teknik Informatika (S1)
77	0333764665130313	MUHAMAD SALMAN ALFARISI	Manajemen Informatika (D3)
78	1961760661130172	MUHAMMAD AINUR RONY	Teknik Informatika (S1)
79	7050757658237093	NAWINDAH	Sistem Informasi (S1)
80	6050754655230123	NIDYA KUSUMAWARDHANY	Sistem Informasi (S1)
81	3547763664230252	NOFIYANI	Sistem Informasi (S1)
82	5037758659230233	NONI JULIASARI	Sistem Informasi (S1)
83	4847756657231432	NURWATI	Sistem Informasi (S1)
84	1834757658230202	PAINEM	Sistem Informasi (S1)
85	2543764665230232	PEPI PERMATASARI	Sistem Informasi (S1)
86	4554760661230252	PIPIN FARIDA ARIYANI	Teknik Informatika (S1)
87	4151756657130113	PURWANTO	Teknik Informatika (S1)
88	8540769670230272	PUTRI HAYATI	Teknik Informatika (S1)
89	2362766667131233	RAHMAT OKTAVIAN	Teknik Informatika (S1)
90	5947771672230352	RATNA KUSUMAWARDANI	Sistem Informasi (S1)
91	3537759660230223	RATNA UJIAN DARI	Sistem Informasi (S1)
92	4656758659230152	RETNO WULANDARI	Sistem Informasi (S1)
93	0949761662230182	REVA RAGAM SANTIKA	Teknik Informatika (S1)
94	0443759660230253	RIRI IRAWATI	Sistem Komputer (S1)
95	1660744645230082	RIRIT ROESWIDIAH	Teknik Informatika (S1)
96	1745767668230302	RISKIANA WULAN	Teknik Informatika (S1)
97	2959764665237002	RIZKA TIAHARYADINI	Teknik Informatika (S1)
98	4456766667130233	RIZKY PRADANA	Sistem Informasi (S1)
99	4943758659130162	RIZKY TAHARA SHITA	Teknik Informatika (S1)
100	6235757658230143	RUSDAH	Ilmu Komputer (S2)
101	6249760661230213	SAFITRI JUANITA	Sistem Informasi (S1)

KAMPUS ROXY MAS : Pusat Niaga Roxy Mas Blok E.2 N0. 38-39 Telp : (021) 6328709, 6328710, Fax : (021) 6322872

KAMPUS SALEMBA MAS : Sentra Salemba Mas Blok S-T, Telp : (021) 3928688, 3928689, Fax : (021) 3161636



No	NUPTK	Nama	Program Studi
102	4554753654230092	SAFRINA AMINI	Teknik Informatika (S1)
103	3444749650130102	SAMIDI	Ilmu Komputer (S2)
104	4261760661230183	SAMSINAR	Sistem Informasi (S1)
105	9937760661130262	SEJATI WALUYO	Teknik Informatika (S1)
106	0157741642130083	SETYAWAN WIDYARTO	Ilmu Komputer (S2)
107	0241752653237043	SRI MULYATI	Sistem Informasi (S1)
108	3542749650230153	SRI WAHYUNINGSIH	Sistem Informasi (S1)
109	0246748649131143	SUBANDI	Teknik Informatika (S1)
110	7944752653130152	SUBANDI	Teknik Informatika (S1)
111	5937767668130372	SYAMSUDIN ZUBAIR	Teknik Informatika (S1)
112	4549736637130032	TATANG WIRAWAN WISNUADJI	Sistem Komputer (S1)
113	5539750651131093	TEJA ENDRA ENG TJU	Sistem Informasi (S1)
114	7552757658230133	TITIN FATIMAH	Sistem Informasi (S1)
115	7449765666230222	TRI IKA JAYA KUSUMAWATI	Sistem Informasi (S1)
116	6447751652130113	UTOMO BUDIYANTO	Teknik Informatika (S1)
117	4639763664130282	WAHYU PRAMUSINTO	Manajemen Informatika (D3)
118	9252739640130053	WENDI USINO	Ilmu Komputer (S3)
119	4749764665137022	WINDARTO	Teknik Informatika (S1)
120	7854758659230162	WINDHY WIDHYANTY	Teknik Informatika (S1)
121	9758748649230072	WIWIN WINDIHASTUTY	Sistem Informasi (S1)
122	2257766667230243	WULANDARI	Sistem Informasi (S1)
123	7863755656130092	YANI PRABOWO	Sistem Komputer (S1)
124	3948765666230332	YESI PUSPITA DEWI	Sistem Informasi (S1)
125	0448750651130092	YUDI SANTOSO	Sistem Informasi (S1)
126	6945763664130252	YUDI WIHARTO	Teknik Informatika (S1)
127	4057766667230303	YULIANAWATI	Sistem Informasi (S1)
128	7061753654230083	YULIAZMI	Sistem Informasi (S1)
129	6952768669130332	ZAQI KURNIAWAN	Teknik Informatika (S1)

Ditetapkan di : Jakarta

Tanggal : 02 September 2025

=====

Dekan Fakultas Teknologi Informasi



Dr. Ir. Achmad Solichin, S.Kom., M.T.I

Design and Simulation Of Hyperspectral Lens System For A Flood Monitoring Cubesat

Audrey Rosadi

Department of Mechanical & Aerospace, Faculty of Engineering
International Islamic University Malaysia
Kuala Lumpur, Malaysia
audrey.padmarini@live.iiu.edu.my

Dwi Pebrianti*

Department of Mechanical & Aerospace, Faculty of Engineering
International Islamic University Malaysia
Kuala Lumpur, Malaysia
dwipebrianti@iiu.edu.my

Luhur Bayuaji

Faculty of Data Science & Information Technology
INTI International University
Nilai, Malaysia
luhur.bayuaji@newinti.edu.my

Indra Riyanto

Faculty of Information Technology
Universitas Budi Luhur
Jakarta, Indonesia
indra.riyanto@budiluhur.ac.id

Abstract—Flooding is one of the most severe environmental disasters, impacting millions of lives and causing significant economic losses. Effective flood monitoring is therefore essential to support timely disaster response, resource management, and damage assessment. However, current optical remote sensing methods to monitor floods, particularly multispectral imaging (MSI), are limited by low spectral resolution and rely heavily on complex post-processing algorithms to extract accurate flood information, leading to higher computational costs and reduced efficiency. To address this limitation, this study presents the hardware design and simulation of a high-resolution hyperspectral lens system optimized for CubeSat deployment. The optical system was modeled and optimized in ANSYS Zemax OpticStudio, targeting a spatial resolution of 30 meters with a 20-degree field of view across 24 spectral bands from 465–810 nm. The final design achieved an effective focal length of 133.394 mm and a total system length of 142.087 mm, with a compact weight of approximately 590 grams, making it suitable for 2U CubeSat integration. Performance analysis confirmed strong imaging quality, with an Airy disk radius of 7.937 micrometers and a Strehl ratio of 0.942. These results demonstrate the system’s capability to deliver high-resolution imaging with minimal reliance on post-processing, offering a compact and efficient optical solution for spaceborne flood monitoring.

Keywords—Hyperspectral Imaging, Lens design, CubeSat, Optimization, ANSYS Zemax OpticStudio.

I. INTRODUCTION

Floods are among the most destructive and frequent environmental disasters, affecting millions of lives and causing major economic losses each year [1]. Water-related disasters made up 73.9% of all natural disasters globally, with over 5,000 such events recorded between 2001 and 2018 [2]. While early detection is crucial, post-flood damage assessment is equally important for guiding emergency response, infrastructure repair, and long-term recovery efforts. High-resolution imaging technologies are particularly valuable in assessing flood-affected areas with greater spatial and spectral detail.

Remote sensing has played a crucial role in advancing flood observation by enabling wide-area coverage through satellite imagery. Conventional systems typically rely on multispectral imaging (MSI), which captures reflected radiation across a few broad spectral bands. While MSI offers

ease of use and rapid data processing, its limited spectral resolution restricts its ability to detect subtle environmental variations, often necessitating extensive post-processing to derive usable flood-related information [3].

Hyperspectral imaging (HSI) captures detailed images across a large number of narrow spectral bands (10–20 nm wide) [4], spanning wavelengths from the visible to the near-infrared (NIR) region [5], as illustrated in Figure 1. This allows for more accurate identification of water presence, flood extent, and changes in land surface and vegetation. HSI’s higher spectral fidelity can reduce dependency on complex processing algorithms and improve the precision of flood mapping and water quality analysis [6].

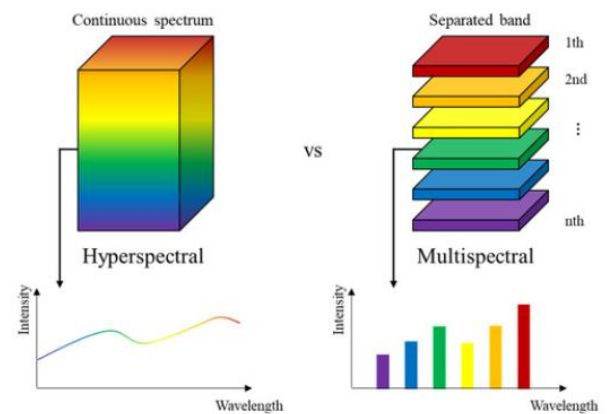


Fig. 1. Spectral Resolution Comparison between hyperspectral and multispectral imagery (Jung et. al., 2024)

However, traditional multispectral and hyperspectral systems are typically mounted on large and costly platforms with limited revisit capabilities. Landsat-8, launched in 2013, is a widely used satellite operating at 705 km in a sun-synchronous orbit. It features the Operational Land Imager (OLI) and Thermal Infrared Sensor (TIRS), capturing visible, NIR, and SWIR bands at 30-meter resolution, a 15-meter panchromatic band, and 100-meter thermal bands (resampled to 30 m). Despite its broad spectral coverage, Landsat-8 relies heavily on post-processing algorithms, such as NDWI, MNDWI, and machine learning classifiers like RBF-SVM, to achieve water detection accuracies above 92%. This

dependence highlights limitations in its raw spectral fidelity. [7].

The ALOS-2 satellite employs PALSAR-2 L-band Synthetic Aperture Radar (SAR), offering high-resolution (~ 3 m) imaging even under cloud cover and dense vegetation. Although its radar-based design ensures day-and-night, all-weather monitoring, its flood detection accuracy remains moderate, averaging around 67.66%. ALOS-2 applies probabilistic modeling and Bayesian inference to support flood simulations, but its performance is constrained by inherent noise in radar backscatter and water differentiation challenges from similar low-reflectance surfaces [8].

The COSMO-SkyMed constellation uses X-band SAR for high-resolution monitoring with a spatial resolution of 0.8×0.8 meters. Its short revisit time enhances temporal monitoring during disasters. For flood detection, COSMO-SkyMed integrates algorithms such as AUTOWADE and ISODATA clustering with spectral indices like NDVI. These techniques enable accurate water area mapping with reported accuracies reaching 90.50%. Despite its strength in rapid monitoring, its reliance on post-processing and environmental correction methods highlights the limitations of raw radar imaging alone for flood delineation [9].

Recent advancements in small satellite platforms, particularly CubeSats, have introduced a scalable, cost-effective alternative for Earth observation missions. CubeSats feature modular construction, faster development cycles, and reduced launch costs, making them ideal for rapid-deployment missions in disaster-prone areas [10]. Despite these developments, existing CubeSat-based flood monitoring missions still rely heavily on limited-spectrum sensors and algorithm-heavy processing. This study aims to address that gap by designing and simulating a compact, high-resolution hyperspectral lens system specifically optimized for CubeSat integration. This work presents a preliminary optical design study focused on lens performance, rather than a complete hyperspectral camera system. By addressing the lens subsystem first, the study establishes a foundation for future integration with sensors, spectral components, and image processing required for full operational deployment.

By focusing on improved optical design at the hardware level, the research seeks to enhance raw image quality, minimize reliance on intensive post-processing algorithms, and support more accurate, efficient flood damage assessment. Through simulation and performance analysis, the proposed system aspires to contribute to more effective damage assessment using spaceborne remote sensing.

II. SETUP AND METHODOLOGY

The optical design and simulation in this study were carried out using ANSYS Zemax OpticStudio 2025 R1 (Student Version), a ray-tracing software widely used for optical system modeling, analysis, and optimization. To guide the system design, key mission functions and operational requirements were first established to ensure that the lens meets the necessary specifications for flood detection and damage assessment, as shown in Table I.

TABLE I. MISSION REQUIREMENTS FUNCTIONS

FUNCTION		OBSERVATION MISSION
Performance	Spatial Resolution	30 m
Spectral Range	Wavelength	465 – 810 nm (24 bands)
Sensor	Hyperspectral Image Sensor	6 μ m
	Ground Sampling Distance (GSD)	30 m
	Scanner Type	Pushbroom
Operating Altitude		700 km
Coverage	Field of View (FOV)	20°
	Latitude coverage	$\pm 98^\circ$
	Swath width	246.86 km
Orbit	Orbit Type	Sun-Synchronous
	Orbital Period	98.62 minutes
	Revisit Time (Single Satellite)	11.11 days

To ensure consistent lighting and global coverage, the hyperspectral lens system is designed for a Sun-Synchronous Orbit (SSO) at 98° inclination [11]. With a 20° field of view, it achieves a swath width of 246.86 km and an orbital period of 98.62 minutes [12]. However, a single satellite offers a revisit time of 11.11 days, which is inadequate for timely flood monitoring. To meet daily observation needs, a constellation of 10–11 CubeSats is proposed, enabling rapid flood detection and enhancing environmental monitoring capabilities [13].

To ensure the effective performance of the hyperspectral system, several key equations have been formulated to define critical parameters as mentioned above. These equations will guide the design process and help optimize the lens system's functionality. The lens system for this research will be modeled for a CubeSat with an altitude of 700 kilometers, image sensor with a pixel size of 6 micrometer, and a refractive index of 1 which represents the space's vacuum. The system will be modeled initially with SCHOTT N-BK7® with a refractive index of 1.517.

$$GSD = \frac{h \times p}{f} \quad (1)$$

where

h = altitude of the satellite (in meters)

s = pixel size of the sensor

f = effective focal length (in meters)

With the focal length f is

$$f = \frac{1}{\phi} \quad (2)$$

where

ϕ = optical power

Optical power ϕ is defined by:

$$\phi = (n_2 - n_1) c \quad (3)$$

where

n = refractive index

c = curvature

And curvature c can be calculated from:

$$c = \frac{1}{R} \quad (4)$$

where

R = radius of the lens

With the parameters defined, the hyperspectral lens system was modeled in Zemax OpticStudio. While the system was dimensioned to meet the requirements for flood detection as one potential use case, no hyperspectral imagery was simulated in this study. Instead, optical performance was evaluated through Zemax's built-in analysis tools and standard RGB test images, which serve only to qualitatively verify imaging quality rather than to replicate mission-specific spectral data. The system was modeled to operate at an altitude of 700 km, with a 10 mm entrance pupil diameter and a total field of view of 20° , sampled at five field angles between 0 and 28.284 mm in 7.071 mm increments. From equation 2, it was discovered that the system's target effective focal length (EFL) is 140 mm. Spectral performance was assessed across 24 wavelengths ranging from 465 nm to 810 nm, covering red-green-blue (RGB) and near infrared (NIR) [14][15][16].

	Wavelength (μm)	Weight	Primary		Wavelength (μm)	Weight	Primary		
<input checked="" type="checkbox"/>	1	0.465	1.000	<input type="radio"/>	<input checked="" type="checkbox"/>	13	0.645	1.000	<input type="radio"/>
<input checked="" type="checkbox"/>	2	0.480	1.000	<input type="radio"/>	<input checked="" type="checkbox"/>	14	0.660	1.000	<input type="radio"/>
<input checked="" type="checkbox"/>	3	0.490	1.000	<input checked="" type="radio"/>	<input checked="" type="checkbox"/>	15	0.675	1.000	<input type="radio"/>
<input checked="" type="checkbox"/>	4	0.510	1.000	<input type="radio"/>	<input checked="" type="checkbox"/>	16	0.690	1.000	<input type="radio"/>
<input checked="" type="checkbox"/>	5	0.525	1.000	<input type="radio"/>	<input checked="" type="checkbox"/>	17	0.705	1.000	<input type="radio"/>
<input checked="" type="checkbox"/>	6	0.540	1.000	<input type="radio"/>	<input checked="" type="checkbox"/>	18	0.720	1.000	<input type="radio"/>
<input checked="" type="checkbox"/>	7	0.555	1.000	<input type="radio"/>	<input checked="" type="checkbox"/>	19	0.735	1.000	<input type="radio"/>
<input checked="" type="checkbox"/>	8	0.570	1.000	<input type="radio"/>	<input checked="" type="checkbox"/>	20	0.750	1.000	<input type="radio"/>
<input checked="" type="checkbox"/>	9	0.585	1.000	<input type="radio"/>	<input checked="" type="checkbox"/>	21	0.765	1.000	<input type="radio"/>
<input checked="" type="checkbox"/>	10	0.600	1.000	<input type="radio"/>	<input checked="" type="checkbox"/>	22	0.780	1.000	<input type="radio"/>
<input checked="" type="checkbox"/>	11	0.615	1.000	<input type="radio"/>	<input checked="" type="checkbox"/>	23	0.795	1.000	<input type="radio"/>
<input checked="" type="checkbox"/>	12	0.630	1.000	<input type="radio"/>	<input checked="" type="checkbox"/>	24	0.810	1.000	<input type="radio"/>

Fig. 2. Wavelength Data

Although this paper focuses on designing a hyperspectral lens system for flood monitoring, it can also be used for vegetation analysis such as Normalized Difference Vegetation Indices (NDVI) and Green Normalized Difference Vegetation Indices (GNDVI), Land Use/Land Cover Classification (LULC), soil and surface analysis, as well as water quality monitoring. This is because the designed lens system incorporates visible (RGB) to near infrared spectral bands.

The initial system incorporated three positive meniscus lenses followed by a triplet with a radius of 70 mm, as calculated from equations 3 and 4, with a minimum lens thickness of 2 mm. This initial design served as the foundation for further optimization. The framework of this study is illustrated in Figure 3.

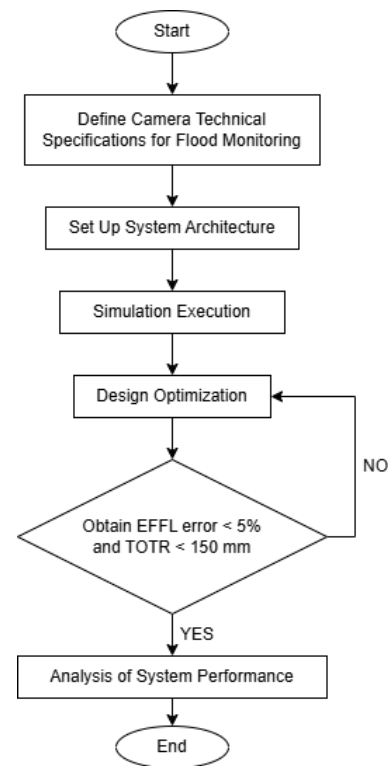


Fig. 3. Flowchart of the Simulation

The system was first aligned using the Quick Focus tool, followed by sequential optimization using local Damped Least Squares (DLS), global Hammer Current DLS, and both local and global Orthogonal Descent (OD) algorithms to refine optical parameters and enhance image quality by adjusting the radii, thicknesses, and materials of each optical element. The finalized optical system comprises three positive meniscus lenses, followed by a doublet and an additional positive meniscus lens, as detailed in Figure 4 [17].

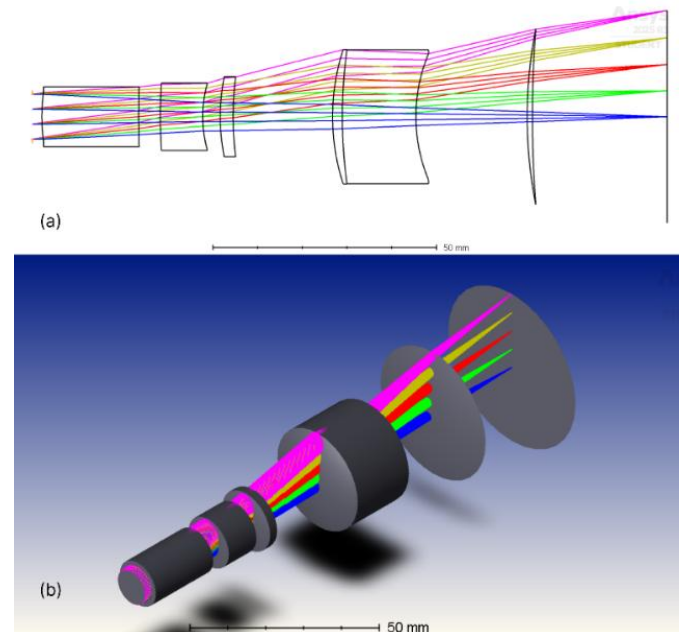


Fig. 4. Optimized Lens System in 2D (a) and 3D Isometric View (b)

The system achieved an effective focal length (EFL) of 133.394 mm, a total optical track length (TOTR) of 142.087 mm, and a total lens assembly weight of 589.975 grams, estimated from the lens materials. Its lens radii, thicknesses, and material selections used in the design are listed in Table II.

TABLE II. FINAL DESIGN LENS DATA

Stop (singlet/doublet)	Inner Radius (mm)	Outer Radius (mm)	Thickness (mm)	Material
First lens (s: singlet)	39.67	309.49	21.67	BAFL4
Second lens (s)	105.93	27.41	9.49	N-SF6
Third lens (s)	44.32	72.21	2.90	KBR
Fourth lens (d: doublet)	48.34	111.36	2.20	ALN
Fifth lens (d)	111.36	36.61	16.46	BAFD7
Sixth lens (s)	101.63	253.47	1.15	EXTEM_XH1015

III. RESULTS AND DISCUSSION

This chapter presents the performance evaluation of the optimized hyperspectral lens system using a series of optical performance metrics. These include spot diagrams, Huygens Point Spread Function (PSF), relative illumination, and image simulation, which collectively assesses the system's imaging quality and alignment with the design objectives.

A. Spot Diagram with Airy Disk Radius

The spot diagram analysis provides insight into the spatial resolution and focusing accuracy of the optimized hyperspectral lens system. It visualizes how rays from a point source converge at the image plane, where a tighter spot distribution means the rays are concentrated closer to the Airy disk radius, indicating sharper and more precise imaging [18].



Fig. 5. Spot Diagram

The spot diagram of the optimized hyperspectral lens system presented in Figure 5 demonstrates a well-controlled distribution of focused light across the field of view. The

RMS spot radius, which measures how tightly rays converge at the image plane, remains close to or smaller than the Airy disk radius of 7.937 μm at 7.273, 7.254, 6.957, and 6.888 μm for 0°, 2.5°, 5°, and 7.5°, respectively. This indicates that at the central to mid field angles, the system is operating near the diffraction limit, delivering sharp, high-resolution imaging. While at 10°, the RMS radius is larger than the Airy disk, at 12.842 μm which suggests some residual aberrations at the edge of the field. Although not diffraction-limited, the system exhibits sufficient focus quality to detect and point out key flood-related features, such as water boundaries, inundation zones, and terrain variations. This level of spatial accuracy supports the system's suitability for flood mapping applications, where consistent image clarity across a wide field is essential for informed decision-making and disaster response.

B. Huygens Point Spread Function (PSF)

To complement the geometric evaluation provided by the spot diagram, the Huygens Point Spread Function (PSF) offers a diffraction-based assessment of the system's performance on how well an optical system focuses light from a point source.

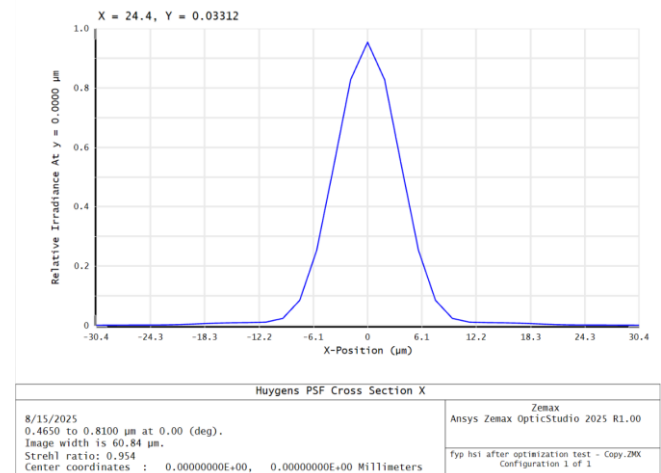


Fig. 6. Huygens PSF

Figure 6 shows the Huygens PSF cross-section of the optimized system, characterized by a sharp central peak with minimal light spread into the surrounding regions. The system achieved a Strehl ratio of 0.954, which is close to the ideal value of 1.0, indicating near-optimum focusing quality and performance close to the diffraction limit. This high concentration of light in the central peak reflects excellent focusing precision, allowing the system to capture fine spatial details with minimal blurring. Such performance demonstrates the lens's capability to deliver sharp, high-contrast images, ensuring reliable optical performance for accurate CubeSat-based flood damage assessment.

C. Relative Illumination

Relative illumination evaluates how evenly light is distributed from the center to the edge of the image field. An

ideal lens system would show a flat line of 1.0 across the field of view.

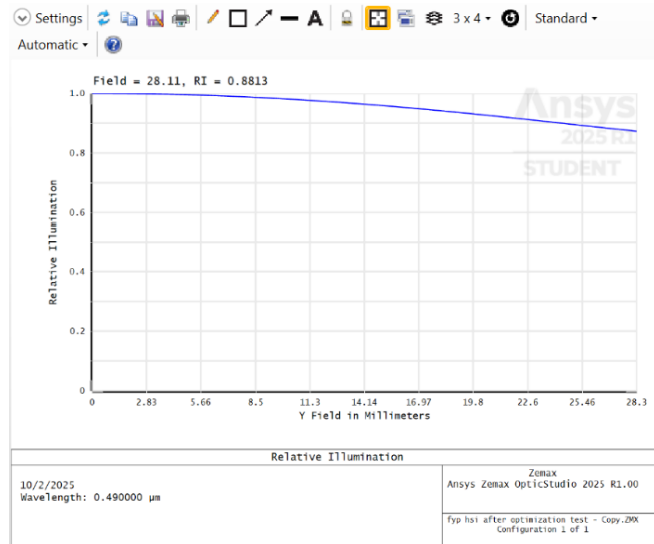


Fig. 7. Relative Illumination

After optimization, illumination remains high across the field, with a slight drop from 1.0 at the center to 0.8813 at the edge, typical of compact optical systems due to vignetting. This fall-off results from prioritizing aberration correction and sharpness, but does not compromise image quality. In flood monitoring, where resolution and clarity are more critical than uniform brightness, this trade-off is acceptable.

D. Image Simulation

The image simulation in this study is based on a standard RGB test image provided within ANSYS Zemax OpticStudio, as hyperspectral image simulation was not supported within the available software environment. The chosen image serves only as a visual reference to assess the optical system's ability to maintain sharpness and contrast after optimization.

The selected image in Figure 8 is a post-disaster flood assessment which occurred in Xaythany, Laos, on July 21, 2025. The image simulated has a size of 36.8661 x 28.2433 mm. This map was prepared by the Mohammed Bin Rashid Space Centre (MBRSC) covering the area of interest (AOI) of 101.793° E to 102.990° E longitude and 19.3123° N to 18.1741° N latitude, extracted from Sentinel 1C. The flooded area in the image is shown in blue.

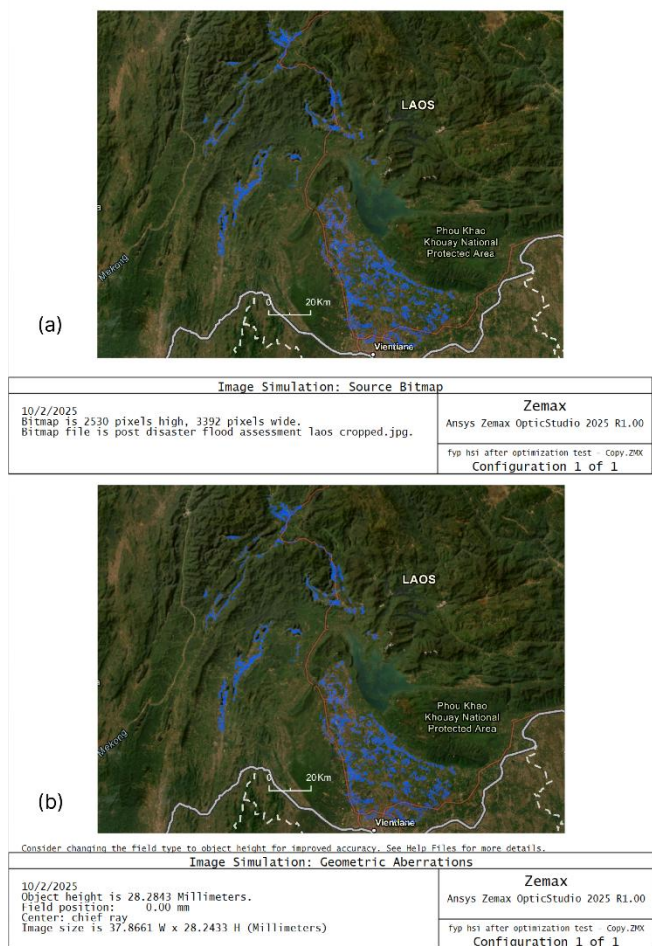


Fig. 8. Flood Assessment in Laos Source Image (a) and Simulation (b) (MBRSC, 2025)

The image simulation in Figure 10 illustrates that the system effectively captures fine image details with sharp focus across the central field and an almost identical contrast retention throughout field angles.

IV. CONCLUSION

This study successfully designed and simulated a high-resolution hyperspectral imaging system optimized for flood detection and monitoring. The final lens system achieved an EFFL of 133.394 mm, with only a 4.72% deviation from the target value, and a total track length of 142.087 mm. The overall weight of the optical assembly is approximately 590 grams, making the system compact and lightweight. These specifications confirm that the design can be effectively integrated into a 2U CubeSat, while allowing space for other essential subsystems.

Performance evaluations confirm the system's suitability for flood monitoring, with the spot diagram and PSF demonstrating strong spatial accuracy and sharp focus across the field. Although a slight decline in relative illumination is observed at the edges, the overall image quality remains high, making the trade-off acceptable for flood monitoring applications.

With this design, it is hoped that flood detection and mapping can be performed more efficiently by reducing reliance on extensive post-processing. This improvement in hardware-level performance is expected to enhance the reliability and responsiveness of satellite-based flood monitoring, supporting more accurate and timely disaster management and recovery efforts.

REFERENCES

- [1] D. Capolongo, A. Refice, and M. Chini, *Improving flood detection and monitoring through remote sensing*. Mdpi AG, 2022.
- [2] J. Lee, D. Perera, T. Glickman, and L. Taing, "Water-related disasters and their health impacts: A global review," *Progress in Disaster Science*, vol. 8, p. 100123, Aug. 2020, doi: 10.1016/j.pdisas.2020.100123.
- [3] S. H. Jung, S. Kwon, I. W. Seo, and J. S. Kim, "Comparison between Hyperspectral and Multispectral Retrievals of Suspended Sediment Concentration in Rivers," *Water*, vol. 16, no. 9, p. 1275, Apr. 2024, doi: 10.3390/w16091275.
- [4] S. Shammi, F. Sohel, D. Diepeveen, S. Zander, and M. G. K. Jones, "A survey of image-based computational learning techniques for frost detection in plants," *Information Processing in Agriculture*, vol. 10, no. 2, pp. 164–191, Feb. 2022, doi: 10.1016/j.inpa.2022.02.003.
- [5] E. R. Reshef, J. B. Miller, and D. G. Vavvas, "Hyperspectral Imaging of the Retina: A review," *International Ophthalmology Clinics*, vol. 60, no. 1, pp. 85–96, Dec. 2020, doi: 10.1097/iio.0000000000000293.
- [6] A. Bhargava, A. Sachdeva, K. Sharma, M. H. Alsharif, P. Uthansakul, and M. Uthansakul, "Hyperspectral imaging and its applications: A review," *Heliyon*, vol. 10, no. 12, p. e33208, Jun. 2024, doi: 10.1016/j.heliyon.2024.e33208.
- [7] I. Ounrit, S. Sinnung, P. Meena, and T. Laosuwan, "Flash Flood Mapping Based On Data From Landsat-8 Satellite And Water Indices," *International Journal on "Technical and Physical Problems of Engineering"*, vol. 14, no. 2, pp. 130–135, Jun. 2022, [Online]. Available: <https://www.iotpe.com>
- [8] M. Ohki, K. Yamamoto, T. Tadono, and K. Yoshimura, "Automated processing for flood area detection using ALOS-2 and hydrodynamic simulation data," *Remote Sensing*, vol. 12, no. 17, p. 2709, Aug. 2020, doi: 10.3390/rs12172709.
- [9] L. Pulvirenti, G. Squicciarino, E. Fiori, L. Candela, and S. Puca, "Analysis and processing of the COSMO-SkyMed second generation images of the 2022 Marche (Central Italy) flood," *Water*, vol. 15, no. 7, p. 1353, Apr. 2023, doi: 10.3390/w15071353.
- [10] S. Mane, Space Nation, and Astroex Research Association, "Theoretical overview on CubeSat Technology," *International Journal of All Research Education and Scientific Methods (IJARESM)*, p. 1107, Jan. 2024, [Online]. Available: <https://www.ijaresm.com>
- [11] Orbital Mechanics for engineering students. 2014. doi: 10.1016/c2011-0-69685-1.
- [12] H. Aboalia, S. Hussein, and A. Mahmoud, *Optimizing High Resolution Wide Field of View Optical Design for Long Wave Infrared Objective*. 2024, pp. 66–71. doi: 10.1109/iceeng58856.2024.10566440.
- [13] P. Gomez, S. A. Leal, L. J. O. Florez, R. A. G. Giraldo, H. Garcia, and H. Arguello, "Design of a Pushbroom NIR Optimized System for Citrus Spectral Data Acquisition," 2024 XVIII National Meeting on Optics and the IX Andean and Caribbean Conference on Optics and Its Applications (ENO-CANCOA), pp. 1–5, Jun. 2024, doi: 10.1109/eno-cancoa61307.2024.10751327.
- [14] S. Dewitte, A. A. A. Nazar, Y. Zhang, and L. Smeesters, "A multispectral camera suite for the observation of Earth's outgoing radiative energy," *Remote Sensing*, vol. 15, no. 23, p. 5487, Nov. 2023, doi: 10.3390/rs15235487.
- [15] C. Pasquini, "Near Infrared Spectroscopy: fundamentals, practical aspects and analytical applications," *Journal of the Brazilian Chemical Society*, vol. 14, no. 2, pp. 198–219, Apr. 2003, doi: 10.1590/s0103-50532003000200006.
- [16] R. Chen et al., "TCNIRV: Topographically Corrected Near-Infrared Reflectance of vegetation for tracking gross primary production over mountainous areas," *IEEE Transactions on Geoscience and Remote Sensing*, vol. 60, pp. 1–10, Jan. 2022, doi: 10.1109/tgrs.2022.3149655.
- [17] R. M. Bunch, *Optical Systems Design detection Essentials*. 2021. doi: 10.1088/978-0-7503-2252-2.
- [18] K. S. Malik, S. Konwar, S. S. G. Buddha, and N. Kumar, *Computation of Spot Diagrams and Ray Tracing of Different Aberrated Beams Using Geometrical Exact Ray Tracing*, vol. 59. 2023, pp. 1–3. doi: 10.1109/wrap59682.2023.10712988.